Journal of Alzheimer's Disease 66 (2018) 1175–1191
DOI 10.3233/JAD-180174
IOS Press

The Ethyl Acetate Extract of Leaves of *Ugni molinae* Turcz. Improves Neuropathological Hallmarks of Alzheimer's Disease in Female APPswe/PS1dE9 Mice Fed with a High Fat Diet

Daniela Jara-Moreno[a,c,e,1], Rubén D. Castro-Torres[a,c,d,f,1], Miren Ettcheto[a,b,c,f], Carme Auladell[d,f], Marcelo J. Kogan[e], Jaume Folch[b,c], Ester Verdaguer[d,f], Amanda Cano[c,g], Oriol Busquets[a,b,c,f], Carla Delporte[e,2] and Antoni Camins[a,c,f,2,*]

[a]*Departament de Farmacologia, Toxicologia i Química Terapèutica, Facultat de Farmàcia i Ciències de l'Alimentació, Universitat de Barcelona, Barcelona, Spain*
[b]*Departament de Bioquímica i Biotecnologia, Facultat de Medicina i Ciències de la Salut, Universitat Rovira i Virgili, Reus, Spain*
[c]*Biomedical Research Networking Centre in Neurodegenerative Diseases (CIBERNED), Madrid, Spain*
[d]*Departament de Biologia Cellular, Fisiologia i Immunologia; Facultat de Biologia, Universitat de Barcelona, Barcelona, Spain*
[e]*Departamento de Química Farmacológica y Toxicológica, Facultad de Ciencias Químicas y Farmacéuticas, Universidad de Chile, Santiago, Chile*
[f]*Institut de Neurociències, Universitat Barcelona, Barcelona, Spain*
[g]*Departament de Farmàcia, Tecnologia Farmacèutica i Fisico-química, Facultat de Farmàcia i Ciències de l'Alimentació, Universitat de Barcelona, Barcelona, Spain*

Accepted 19 September 2018

Abstract. The most common type of dementia is Alzheimer's disease (AD), a progressive neurodegenerative disease characterized by impairment in cognitive performance in aged individuals. Currently, there is no effective pharmacological treatment that cures the disease due to the lack of knowledge on the actual mechanisms involved in its pathogenesis. In the last decades, the amyloidogenic hypothesis has been the most studied theory trying to explain the origin of AD, yet it does not address all the concerns relating to its development. In the present study, a possible new preclinical treatment of AD was evaluated using the ethyl acetate extract (EAE) of leaves of *Ugni molinae* Turcz. (synonym *Myrtus ugni Molina* Family Myrtacea). The effects were assessed on female transgenic mice from a preclinical model of familial AD (APPswe/PS1dE9) combined with a high fat diet. This preclinical model was selected due to the already available experimental and observational data proving the relationship between obesity, gender, metabolic stress, and cognitive dysfunction; related to characteristics of sporadic AD. According to chemical analyses, EAE would contain polyphenols such as tannins, flavonoid derivatives, and

[1]These authors contributed equally to this work.

[2]These authors contributed equally as senior authors.

*Correspondence to: Antoni Camins PhD, Departament de Farmacologia, Toxicologia i Química Terapèutica, Facultat de Farmàcia i Ciències de l'Alimentació, Universitat de Barcelona, Avda/ Diagonal 643, E-08028 Barcelona, Spain. Tel.:+34 93 4024531; Fax:+34 934035982; E-mail: camins@ub.edu.

phenolic acids, as well as pentacyclic triterpenoids that exhibit neuroprotective, anti-inflammatory, and antioxidant effects. In addition, the treatment evidenced its capacity to prevent deterioration of memory capacity and reduction of progression speed of AD neuropathology.

Keywords: APPswe/PS1dE9, ethyl acetate extract, high fat diet, hippocampus, neuroinflammation, Ugni molinae

INTRODUCTION

Alzheimer's disease (AD) is an irreversible, chronic, and relentless neurodegenerative disease, characterized by memory loss, psychoses, and affective disorders and behavioral alterations [1–5]. Multiple epidemiological studies have estimated that the incidence of AD is expected to increase to 66 million diagnosed cases in the world by 2030 and 131 million by 2050. These values are the result of increase in life expectancy and continuous aging of developed societies. Nowadays, there are no curative therapies for AD [1, 3] and the drugs being administered are only able to slow the progression of the disease for a reduced period of time [1]. Also, they present variable effectiveness depending on the individual characteristics of the patient and their efficacy decreases as the disease progresses [6–8].

The well-known neuropathological features observed in AD brains include the presence of extracellular amyloid-β (Aβ) plaques/deposits intracellular neurofibrillary tangles (NFTs) and synaptic dysfunction [9–14]. In addition, many reports evidence a role of activated glia and its pro-inflammatory mediators in the etiology of AD [15–18]. Although the precise role of inflammatory processes in AD pathophysiology is controversial, it is believed that microglia and astrocytes become activated, promoting the secretion of cytokines and neurotoxic mediators, including tumor necrosis factor alpha (TNF α), superoxide ($O^{2-\bullet}$), and nitric oxide (NO), which exacerbate neuronal damage [15]. Thus, several authors have hypothesized that AD could be described as a chronic brain inflammatory disease [18]. Nonetheless, other elements have been suggested as risk factors for the development of late onset AD. Among them, the most considered are age and vascular and metabolic disorders such as hypertension, type II diabetes mellitus (T2DM), dyslipidemia, and metabolic syndrome [19–23].

U. molinae is a native and wild shrub of the Myrtaceae family. It grows in central-south Chile (between the VII and X region), especially in the Coast Mountains and in part of the pre-Andean mountains. In Chilean folkloric medicine, the aerial parts and its infusions have been used to treat urinary infections, diabetes, inflammatory states and different types of pain. Also, analgesic and anti-inflammatory properties have been demonstrated by *in vivo* assays using the extracts of *U. molinae* leaves [24–28]. In these studies, it was determined that these effects are due to the presence of phenolic compounds: genins and heterosides of quercetin, kaempferol, myricetin, epicatechin/catechin; gallic acid, quinic acid, tannins and others similar compounds and pentacyclic triterpenoids from ursane, oleanane and lupane cores (Fig. 1A, B) [24–28].

Given the previous assumption on the important role of inflammation in the development of AD-like pathologies, in this study a familial model of the disease was used to study the efficacy of the extract from *U. molinae* as a novel disease-modifying treatment. Likewise, since experimental preclinical reported studies strongly suggest that obesity and T2DM conditions might aggravate AD pathologies, the variable of a high-fat diet (HFD) was included [29–34].

MATERIALS AND METHODS

Plant material

U. molinae leaves were collected and botanically identified by Dr. Carla Delporte in April 2010, in south-central Chile (35°45´S, 72°33´W). A voucher specimen was deposited in the herbarium of the School of Chemical and Pharmaceutical Sciences, University of Chile (SQF: 22462). Dried and grinded leaves (2.0 kg) were successively treated for extraction by maceration at room temperature with hexane, dichloromethane, ethyl acetate, and ethanol to obtain, after the concentration, the corresponding dry extracts with a w/w yield of 1.4, 5.9, 3.7, and 22.2%, respectively. The selected ethyl acetate extract (EAE) was dissolved in dimethyl sulfoxide and later it was diluted in saline solution (NaCl 0.9% p/p) to inject at a dosage of 30 mg/kg of mice.

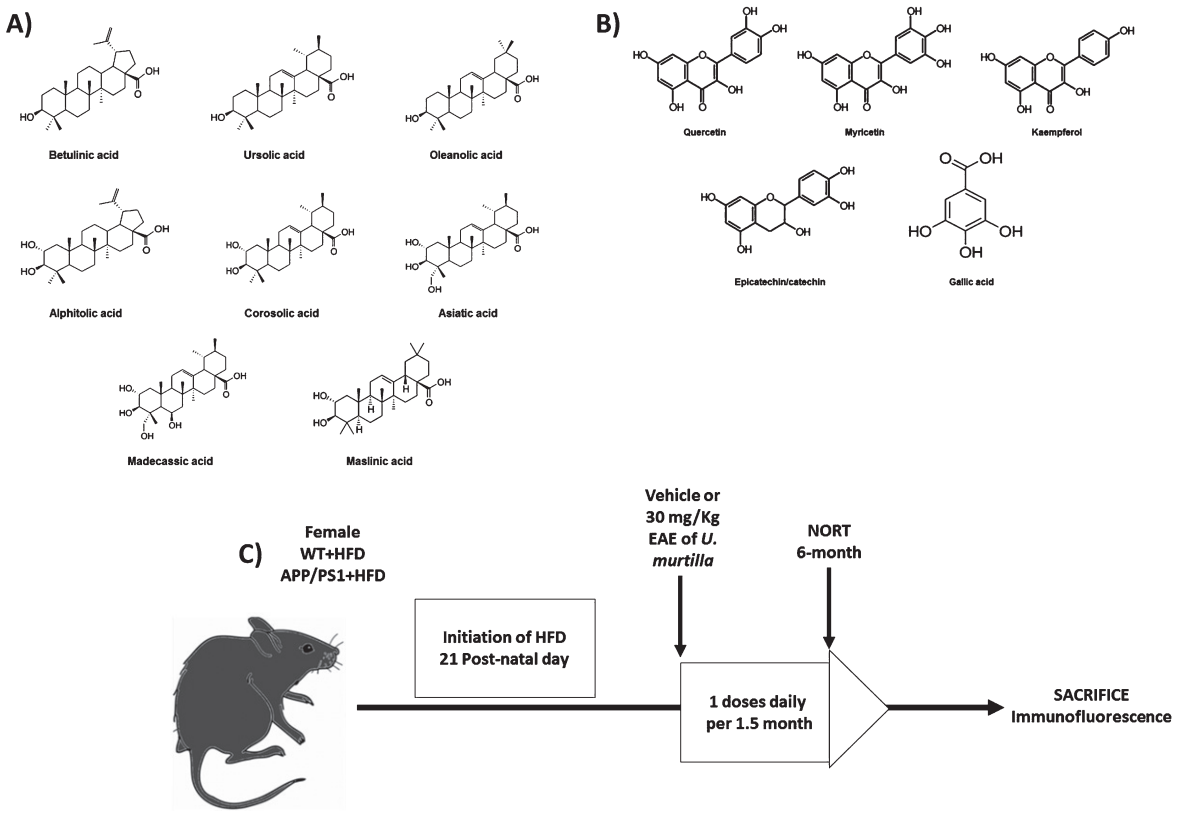

Fig. 1. Chemical structure of several compounds present in EAE of *U. molinae* leaves. A) Polyphenolic compounds. B) Pentacyclic triterpenoids. C) Experimental design for this study. Female WT and APP/PS1 mice were used in this study. All animals were exposed to HFD right after their weaning and, from the 4.5 months of age they were administered either the vehicle or EAE extract at 30 mg/kg daily. At 6 months of age all animals underwent the NORT and were sacrificed in order to obtain samples for IF assays.

Chemical characterization of EAE

Total phenolic content

The total phenolic content (TPC) was determined by Folin Ciocalteau assay according to Peña-Cerda et al. [25]. Briefly, EAE was dissolved in methanol: water (2 : 8) and 30 μL of sample was mixed with 30 μL Folin Ciocalteau reagent (1 : 10 in water). Then 240 μL of sodium carbonate (5% v/v) was added. Finally, the detection was made at 40°C in a 96-well plate spectrophotometer (Multiskan GO, Thermo Scientific, USA) and the absorbance was measured at 765 nm after 20 min of reaction. A calibration curve was made with gallic acid ($y = 0.062x+0.053$, $R^2 = 0.998$ and $F_{calc} = 0.30 < F_{tab}=3.71$) as standard compound. The TPC was expressed as mg gallic acid per g dry extract.

Total flavonoid content

The total flavonoid content (TFC) was calculated by an $AlCl_3$ complexation method according to Peña-Cerda et al. [25]. Briefly, EAE was dissolved in methanol and 30 μL of sample was mixed with 10 μL of sodium acetate (1 M) and 240 μL of distilled water. The method was performed at room temperature in a 96-well plate spectrophotometer under a 415 nm wavelength, 30 min after the beginning of the reaction. A calibration curve was made with quercetin as standard compound ($y = 0.049x + 0.003$, $R^2 = 0.999$ and $F_{calc} = 0.06 < F_{tab} = 3.49$) and TFC was expressed as mg quercetin per g dry extract.

Identification of phenolic compounds by mass spectrometry

Methanolic solutions of EAE (5000 ppm) were prepared and HPLC-UV-ESI-MS analyses were performed to obtain the polyphenolic fingerprint of this extract. The HPLC system was an Agilent 1100 (Agilent Technologies Inc., CA-USA) coupled with an electrospray ion trap mass spectrometer Esquire 4000 ESI-IT (Bruker Daltonics GmBH, DE). Analyses and UV detection were made at 270 and 360 nm

correspondingly. HPLC separation was carried out on a reverse phase Purospher® STAR RP-18 column (endcapped 5 μm, Hibar® RT 250–4; Merck, Darmstadt, Germany). Methanolic solution of EAE was separated by HPLC gradient elution which was established by mixing two mobile phases: phase A (H_2O/HCOOH 98 : 2) and phase B (H_2O/CH_3CN /HCOOH 18 : 80 : 2), according to methodology used by Michodjehoun-Mestres et al. [35]. The elution's run time was 90 min and the gradient elution was: 0–8 min 90% A, 8–45 min 84% A, 45–55 min 65%A, 55–72 min 20% A, 72–75 min 0% A, 75–78 min 95% A, 80–90 min 90% A at a flow rate of 0.2 mL/min. The ionization (nebulization) was performed by an electrospray ionizator and an ion trap was used as mass analyzer. Negative polarity was employed in ESI. The following parameters were considered for mass spectrometry: spray ionization voltage was 4000 V; nitrogen (N_2) was used as nebulizer gas; temperature was 365°C; pressure 45 psi; and flow rate 10 L/min. Data was analyzed using Data Analysis Version 3.2 software (Bruker Daltonik GmbH, Germany). Compound identification was done using Mass Bank database or by comparison with scientific literature.

Animals

Female APPswe/PS1dE9 (APP/PS1) and C57BL/6J *wild-type* (WT) mice were used in this study. APP/PS1 animals co-express a Swedish (K594M/N595 L) mutation of a chimeric mouse/human amyloid precursor protein (APP), together with the human exon-9-deleted variant of presenilin 1 (PS1). Both mutations are associated with AD and represent a preclinical model to study some of the features of familial AD. The animals were originally purchased from Jackson Lab (https://www.jax.org/strain/004462). The original background is (C57BL/6 x C3 H)-F_2. Thus, living colony in our facilities are currently maintained as hemizygote against C57BL/6J for at least 8 generations.

The mice were fed for 6 months with either control (CT) or HFD (D08061110; Research Diets Inc., New Brunswick, USA). This diet is enriched with hydrogenated coconut oil, increasing fat content up to 45% (Table 1). Mice body weight was recorded weekly from the beginning of treatment (4.5 months old) until their sacrifice at 6 months of age. Animals that underwent the treatment with EAE were injected intraperitoneally (i.p.) daily from the 4.5 months of age until their sacrifice at 6 months of age. These time periods were chosen in order to present the treatment as a prevention and possible reversal method of the negative neuropathophysiology of AD. EAE was administered at a dosage of 30 mg/kg given the maximum possible dissolution rate between dimethyl sulfoxide and saline solution. The control mice were injected with analogue proportions of dimethyl sulfoxide diluted with saline solution.

Table 1
Composition of High Fat Diet

	Kcal %
Proteins	16.4
Carbohydrates	38.6
Fats (coconut oil)	45.0
Total	100.0

Twenty-five animals were used in total, divided into four groups: WT+HFD, APP/PS1 + HFD, WT+HFD+EAE, and APP/PS1 + HFD+EAE. Groups WT+HFD and APP/PS1 + HFD were administrated with the vehicle where EAE was dissolved. The experimental design is represented in Fig. 1. All the animals were kept under controlled temperature, humidity, and 12 h light/dark conditions with food and water provided *ad libitum*. In all situations, mice were treated in accordance with the European Community Council Directive 86/609/EEC and the procedures established by the Department d'Agricultura, Ramaderia i Pesca of the Generalitat de Catalunya. Every effort was made to minimize animal suffering and to reduce the number of animals used. Following *in vivo* testing, the animals were sacrificed and all mice were used for immunohistochemistry (IHC) microscopy analysis.

Glucose Tolerance Test (GTT) - Insulin Tolerance Test (ITT)

Before starting the treatment with EAE, the animals underwent a GTT and ITT test to determine whether their metabolic state has acquired a diabetogenic/obesogenic profile. Animals were fasted for 6 h previous to the intraperitoneal (i.p.) administration of either substance. In GTT mice were injected a glucose dosage of 1 g/kg, whereas in ITT, insulin was administered at a dosage of 0.75 ui/kg ratio. Next, blood samples were analyzed from the tail vein in consecutive time periods. For GTT samples were extracted at 5, 15, 30, 60, 120, and 180 min after the administration; in ITT measurements were made 15, 30, 45, 60,and 90 min after. Animals were continuously observed and monitored and, in those cases in which

glucose dropped under a concentration of 20 mg/dL, animals were administered a glucose dosage of 1 g/kg and kept under observation until glucose blood levels stabilized and normal behavior was observed.

Novel Object Recognition Test (NORT)

The Novel Object Recognition Test was used to evaluate hippocampal-dependent recognition memory of mice [35]. The task procedure consisted of three phases: habituation, familiarization and probe. In the habituation phase, mice explored individually a circular open-field arena of 40 cm of diameter for three consecutive days, 10 min for each session. On the fourth day (familiarization), each mouse was placed in the arena containing two identical objects ($A + A$) in the middle of the field for 10 min. To perform the test phase, mice were returned 24 h later to the open-field with two objects, one was identical to the day before and the other was a novel object ($A + B$) for 10 min. Light intensity was kept constant in all phases and the arena and objects were cleaned with 96° ethanol between each animal to eliminate olfactory cues. Exploration activity was defined as the orientation of snout of the animals toward the object, sniffing or touching. The exploratory analysis was expressed as discrimination index (DI). DI=(novel object exploration time/total exploration time) – (familial object exploration time/total exploration time), measured in seconds.

Immunohistochemistry

Mice used for IHC studies were anesthetized by i.p. injection of sodium pentobarbital (80 mg/kg) and intracardiacally perfused with 4% paraformaldehyde (PFA) diluted in 0.1 M phosphate buffer (PB). Brains were removed and stored in the same solution overnight (O/N) at 4°C and then, they were cryoprotected in 30% sucrose-PFA-PB solution. Samples were frozen at –80°C and coronal sections of 20 μm of thickness were obtained by a cryostat (Leica Microsystems, Wetzlar, Germany) and kept in cryoprotectant at –20°C until use.

Free-floating sections were first washed three times with 0.1 mol/L PBS pH 7.35 and, after, five times with PBS-T (PBS 0.1 M, 0.2% Triton X-100). Then, they were incubated in a blocking solution containing 10% fetal bovine serum (FBS), 1% Triton X-100 and PBS 0.1 M- 0.2% gelatin for 2 h at room temperature. After that, slices were washed with PBS-T (PBS 0.1 M, 0.5% Triton X-100) five times for 5 min each and incubated with polyclonal rabbit anti-Glial Fibrillary Acidic Protein (GFAP; 1 : 2000; Dako, Glostrup, Denmark), rabbit anti-Ionized calcium-binding adapter molecule (IBA1; 1 : 1000; Wako Chemical USA), and mouse anti-$A\beta_{1-42}$ (12F4; 1 : 1250; Covance, USA) primary antibodies at 4°C O/N. Sequentially, sections were washed with PBS-T (PBS 0.1 M, 0.5% Triton X-100) 5 times for 5 min and incubated with Alexa Fluor 594 goat anti-rabbit and Alexa Fluor 488 donkey anti-rabbit secondary antibodies (1 : 500; Invitrogen, Eugene, OR, USA) for 2 h at room temperature in the dark.

The staining for plaques was performed using Thioflavin S (ThS 0.002%, Sigma-Aldrich) in a 0.033% dilution rate. Slices were incubated for 8 min in the dark, washed with ethanol 50% twice for 1 min and rinsed with PBS 0.1 M. Later, sections were co-stained with 0.1 μg/mL Hoechst 33258 (Sigma-Aldrich, St Louis, MO, USA) for 15 min in the dark, and washed with PBS 0.1M. Finally, the slices were mounted using Fluoromount G (EMS) and the image acquisition was performed with an epifluorescence microscope (BX41 Laboratory Microscope, Melville, NY-Olympus America Inc.).

Image analysis and quantification

We analyzed the cortex in brain coronal sections obtained from Bregma –1.28 to –2.12 mm, in accordance with the Paxinos and Franklin atlas [36]. The analysis and quantification of IHCs and ThS staining were performed using images obtained with the 20x objective. 4–8 sections/animal from 4–6 animals/group were used in all quantifications, except for particle analysis (3 animals/group).

Evaluation of astrocyte and microglia reaction

The quantification of astrocyte and microglia reaction was performed with GFAP and IBA1 markers. The immmunopositive reactivity of the tissue were done through the percentage area occupied by

Table 2
Content of pentacyclic triterpenoid in EAE (30 mg/Kg)

Pentacyclic triterpenoid	%w/w
Madecassic acid	0.33 ± 0.09
Asiatic acid	2.43 ± 0.09
Alphitolic acid	2.82 ± 0.09
Corosolic acid	8.28 ± 0.21
Maslinic acid	2.25 ± 0.12
Betulinic acid	0.54 ± 0.21
Oleanolic/ursolic acid	6.27 ± 0.06

fluorescent signal as previously described by de Lemos et al. [37]. Briefly, images were captured and calibrated using a scale. Then, were transformed to 8-bits gray, inverted and highlighted the area occupied by fluorescent signal (IBA1 or GFAP cells) under fixed threshold using the NIH ImageJ software.

Evaluation of cortical Aβ load

To evaluate the number of Aβ plaques and their size (μm^2) C*ell counter* and *particle quantification* Image J functions were used. $A\beta_{1-42}$ density of aggregates were evaluated using both fluorescent IHC (12F4) and ThS staining. Intensity was determined as follows: Area of fluorescent signal (μm^2) / Total analyzed area. It was expressed as % area.

Gliosis surrounding amyloid plaque

To quantify the astrocytes surrounding Aβ plaques, different plaques per tissue section using superimposed grid of $200 \times 200\ \mu m^2$ were used. Aβ plaques were put in the center of the grid and then channels were spliced using Image J. The size of GFAP positive cells was determined using *particle quantification* of Image J. Particles with GFAP immunoreaction minor than $5\ \mu m^2$ were considered artefacts and therefore were excluded from the analysis. In order to identify if there was gliosis around the plaques the ratio between GFAP area surrounding the plaque and the area of this plaque was calculated.

Microglial reactivity was evaluated by analyzing microglial areas around $A\beta_{1-42}$ aggregates. To do that, double IHC against IBA1 and $A\beta_{1-42}$ peptides (12F4) were used. From cortical sections, the area

Table 3
EAE (270 nm). Identification of phenolic compounds by HPLC-UV-ESI-MS^2 (ESI-IT)

Compound	T_r (min)	MW (g/MOL)	$[M-H]^-$ (m/z)	MS^2 (m/z)	Reference
1. Stricnin/isostricnin isomer (galloyl-HHDP-hexose)	3.7	634	633	300 274 420	a
2. Pedunculagin I/casuariin isomer (bis-HHDP-hexose)	3.7	784	783	300 481	a
3. Digalloyl glucose isomer (digalloyl hexose)	3.7	484	483	331 169	a
4. Gallic acid	4.0	170	169	125	b
5. Stricnin/isostricnin isomer (galloyl-HHDP-hexose)	6.4	634	633	300 274 420	a
6. Digalloyl glucose isomer (digalloyl hexose)	7.0	484	483	331 169	a
7. Pedunculagin I/casuariin isomer (bis-HHDP-hexose)	10.1	784	783	481 301	a
8. Digalloylquinic acid	10.5	496	495	343 325 169	a
9. Pedunculagin I/casuariin isomer (bis-HHDP-hexose)	11.4	784	783	481 300	a
10. Digalloyl glucose isomer (digalloyl hexose)	11.4	484	483	331 169	a
11. Pedunculagin I/casuariin isomer (bis-HHDP-hexose)	11.4	784	783	300 481	a
12. Digalloyl glucose isomer (digalloyl hexose)	12.8	484	483	331 169	a
13. Digalloyl glucose isomer (digalloyl hexose)	14.3	484	483	331 169	a
14. Digalloyl glucose isomer (digalloyl hexose)	16.0	484	483	169 331	a
15. Epicatechin/catechin	15.6	290	289	244 204 178	b
16. Trigalloyl hexose isomer	17.0	636	635	464 482 313	a
17. Myricetin galloyl hexoside	18.3	632	631	478 316	a
18. Trigalloylquinic acid	18.1	648	647	476 325	a
19. Flavogalonic dilactone acid isomer	18.7	470	468	450 425 300	a
20. Flavogalonic dilactone acid isomer	20.2	470	468	425 300 450	a
21. Myricetin galloyl hexoside	20.4	632	631	479 316	a
22. Digalloyl pentose	20.6	454	453	313 168 326	a
23. Myricetin galloyl hexoside	23.9	632	631	479 316	a
24. Myricetin deoxihexoside	26.7	464	463	317 463	a
25. Myricetin hexoside	28.0	480	479	316 179 271	b
26. Myricetin deoxihexoside	28.5	464	463	463 317 179	a
27. Quercetin galloyl hexoside (galloylquercetin)	31.6	616	615	463 301	a
28. Quercetin pentoside	33.0	433	433	301 150	a
29. Myricetin pentoside	34.3	450	449	318 179 152	b
30. Ellagic acid	35.5	302	301	300 228 185	a
31. Ellagic acid	36.2	302	301	300 228 185	a
32. Kaempferol galloyl hexoside	38.4	600	599	447 312 284	a
33. Quercetin pentoside	45.0	434	433	300 179	a
34. Quercetin deoxihexoside	48.8	448	447	447 301	a
35. Myricetin galloyl deoxihexoside	55.6	616	615	616 316 462	a
36. Quercetin	63.7	302	301	178 150 300	b

a, scientific article; b, database; T_r, retention time; MW, molecular weight; EAE, ethyl acetate extract.

Table 4
EAE (360 nm). Identification of phenolic compounds by HPLC-UV-ESI-MS^2 (ESI-IT)

Compound	T_r (min)	MW (g/mol)	[M-H] $^-$ (m/z)	MS^2 (m/z)	Reference
1. Digalloyl hexose isomer	14.4	484	483	313 331 169	a
2. Epicatechin/catechin	15.6	290	289	205 245 137	a, b
3. Digalloyl pentose	15.6	454	453	313 169	a
4. Trigalloylquinic acid	17.7	648	647	495 477	a
5. Trigalloyl hexose isomer	17.9	636	635	465 483 423	a
6. Trigalloylquinic acid	18.6	648	647	495 477	a
7. Trigalloyl hexose isomer	19.2	636	635	465 483 423	a
8. Flavogalonic dilactone acid isomer	20.1	470	468	425 450	a
9. Digalloyl pentose	20.5	454	453	313 169	a
10. Myricetin galloyl hexoside	23.5	632	631	479 316	a
11. Quercetin galloyl hexoside	31.5	616	615	615 463 301	a
12. Quercetin galloyl hexoside	33.2	616	615	615 463 301	a
13. Ellagic acid	35.3	302	301	301 229 185	a
14. Ellagic acid	36.2	302	301	301 229 185	a
15. Kaempferol galloyl hexoside	38.2	600	599	447 285 313	a
16. Quercetin pentoside	44.7	434	433	300 179 150	b
17. Quercetin pentoside	45.7	434	433	300 179 150	b
18. Quercetin hexoside	48.6	448	447	300 179 284 271	a
19. Myricetin galloyl deoxihexoside	53.8	616	615	615 316 463	a
20. Myricetin	53.6	318	317	178 150	b
21. Myricetin galloyl deoxihexoside	55.4	616	615	615 463 317	a
22. Myricetin galloyl deoxihexoside	55.8	616	615	615 316 463	a
23. Quercetin	63.6	302	301	178 150 301	b

a, scientific article; b, database; T_r, retention time; MW, molecular weight; EAE, ethyl acetate extract.

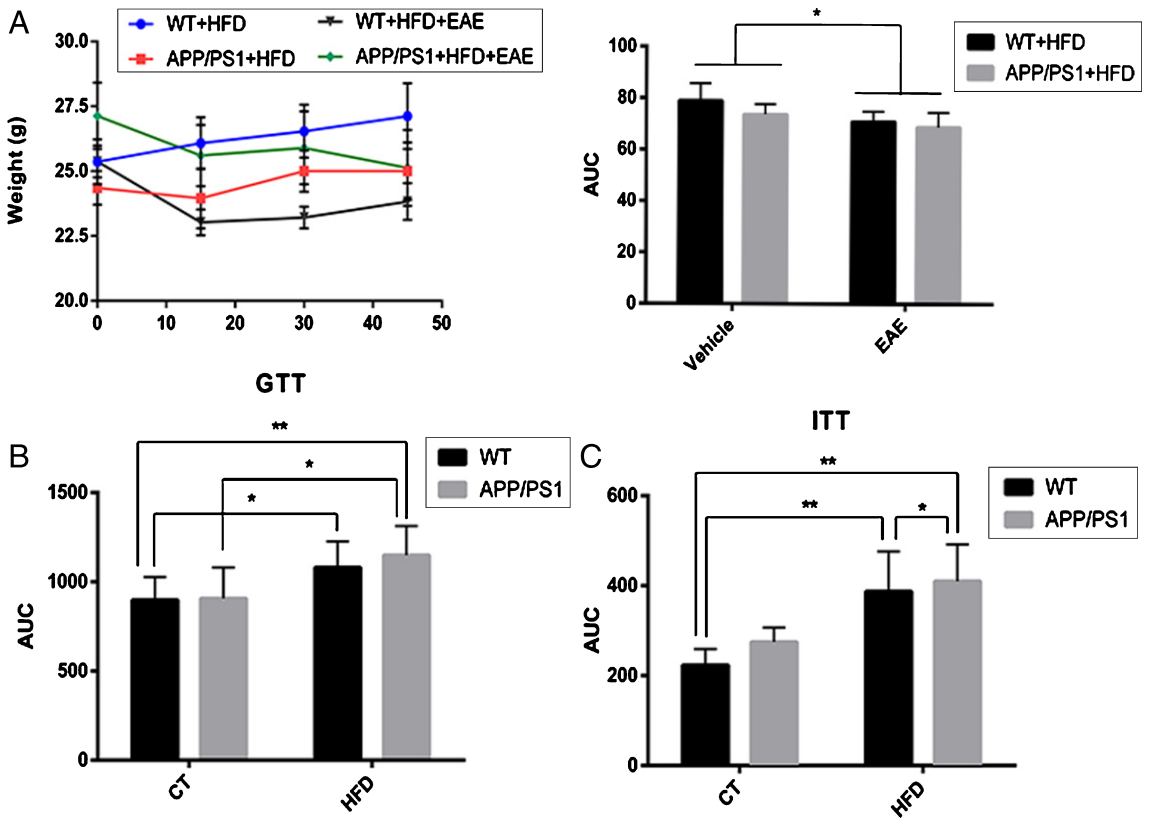

Fig. 2. Peripheral metabolic parameters in HFD-fed WT and APP/PS1 mice. Weekly bodyweight variation (A), GTT (B), and ITT (C) in 6-month-old mice ($n = 5$–12 independent samples per group). For the ITT and the GTT, AUC data were calculated from the time point 0 till the end of the experiment. The results were presented as MEAN ± SEM. Statistical analysis was performed by two-way ANOVA test, with Tukey´s *post hoc* test where $^*p < 0.05$ and $^{**}p < 0.01$.

occupied by the fluorescent signal from their correspondent channel (green = IBA1; red = $A\beta_{1-42}$) and the ratio of IBA1/$A\beta_{1-42}$ were calculated.

Data analysis

All data is presented as mean alone or mean ± SEM. Level of significance was fixed at α=0.05. Thus, calculated p-values<0.05 were considered significant. Differences between samples/animals were evaluated using either two-way ANOVA with Tukey's and unpaired Student-t as required. Both statistical analyses and graphs presented here were created with the Graph Pad InStat software V5.0 (Graph Pad Software Inc., San Diego, CA, USA).

RESULTS

Chemical characterization of EAE

EAE is composed of pentacyclic triterpenoids. They were quantified according to Goity et al. [28] (Table 2): corosolic and oleanolic/ursolic mixtures (8.28 ± 0.21% and 6.27 ± 0.06, respectively) were the most abundant triterpenoids in this extract. Also, the polyphenolic content of EAE was 75.05 ± 5.73 mg gallic acid equivalents/g dry extract (2.25 ± 0.17 mg gallic acid equivalents/g dry extract in the administrated dose, 30 mg/Kg). Additionally, the flavonoid content of EAE was 27.7 ± 5.3 mg quercetin equivalents/g dry extract. Moreover, additional polyphenolic derivatives using mass spectrometry were identified: tannins as gallotannins (di- and tri-galloyl derivatives), ellagitannins (hexahydroxydiphenoyl (HHDP) and hexose derivatives), and quinic acid derivatives. Also, flavonoids as myricetin, quercetin, kaempferol, epicatechin/catechin, its heterosides, and phenolic acids as gallic and caffeic acids derivatives were identified (Tables 3 and 4).

Treatment with EAE avoids weight gain due to HFD and improves cognitive function in APP/PS1 + HFD mice.

Our data showed that EAE treatment decreases body weight significantly in both genotypes, WT and APP/PS1 (F (1, 34)=17.48; p = 0.0002) (Fig. 2). As expected, HFD intake induced significant increases in glucose plasma levels in the GTT and ITT tests,

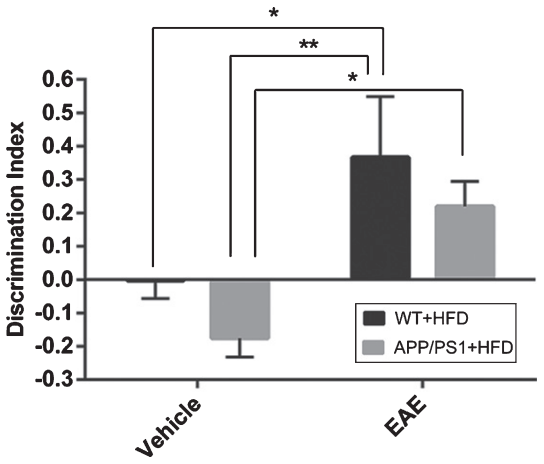

Fig. 3. Graphical representation on the results of the NORT. The results exemplify the beneficial effects of EAE on the WT+HFD+EAE and APP/PS1 + HFD+EAE experimental groups. Values were calculated according to the following formula: Discrimination ratio = (Time spent exploring the new object – Time spent exploring the known object)/Total exploration time. Results were represented as MEAN ± SEM. Statistical analysis was obtained from a two-way ANOVA test followed by a Tuckey's *post-hoc* ($^{*}p < 0.05$ and $^{**}p < 0.01$).

Table 5
Time of exploration (seconds) recorded in these study

	A object	B object		A object	B object
WT HFD	3.09	3.54	APP/PS1 + HFD	9.50	4.80
	2.23	1.85		1.87	2.19
	3.09	3.71		6.00	3.00
	6.83	5.64		39.20	33.50
	0.71	0.76		2.19	2.07
	1.10	0.651	WT+HFD+EAE	6.34	7.26
	5.53	4956		5.25	4.81
	8.30	8.60		3.22	7.20
	17.30	26.90		0.12	9.50
	0.60	1.00		3.05	7.64
	1.00	1.60	APP/PS1 + HFD+EAE	1.37	3.8
	1.80	1.50		4.68	6.59
	1.90	1.3		3.32	5.80
	1.60	6.40		5.34	6.08
	0.80	0.30		11.34	13.07
	2.60	3.60		3.54	5.45
	0.70	0.40			

analyzed by two-way ANOVA (F(1, 42)=17.81; p = 0.001, F(1, 24)=23.49; $p < 0.0001$), respectively.

Furthermore, EAE treatment significantly improved cognitive performance when evaluating using the behavioral NORT (F (1, 34)=17, 48; p = 0.002) (Fig. 3). It can be observed that in APP/PS1 + HFD transgenic mice that there was a significantly reduction versus WT+HFD

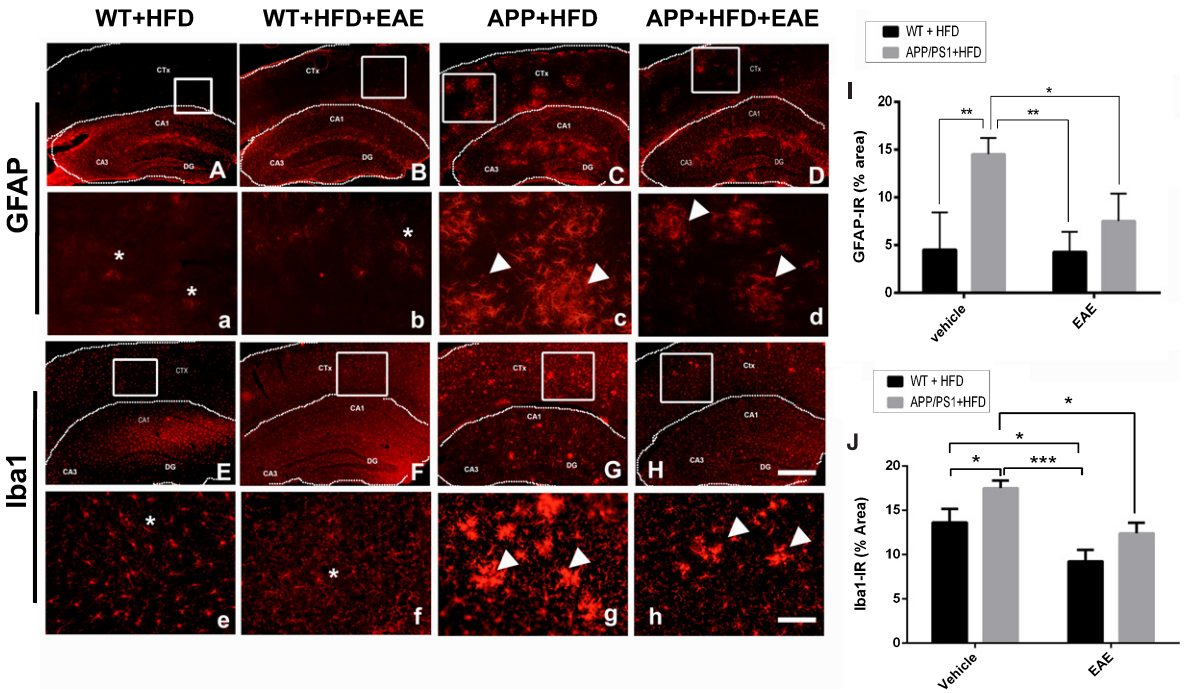

Fig. 4. Fluorescent IHC against GFAP (A, a, B, b, C and c) and IBA1 (E, e, F, f, G and g) in the cortex of the mice untreated and treated with EAE. Low astrocytic reactivity in WT+HFD (A, a) and WT+HFD+EAE (B, b) mice (* indicate astrocytes). As is observed in E there is a microglial reactivity in WT+HFD (*, E, e) and a softly reduction of the reactivity due to EAE in WT+HFD+EAE (*, F, f). Meanwhile, transgenic APP/PS1 + HFD mice show a reactive morphology of astrocytes (arrowheads, C, c) and microglia (arrowheads. G, g) surrounding plaques. A reduction in astrocyte (D, c) and microglial (F, f) reactivity is observed in the APP/PS1 + HFD mice treated with EAE (arrowheads). Quantification of GFAP (J) and IBA1 (K) positive cells is shown in the graph bars. Graphs represent the mean ± SEM. (*$p<0.05$, **$p<0.01$, ***$p<0.001$) Abbreviations: CTx, cortex; CA1, cornu ammonis; DG, dentate gyrus. Scale bar for A. B. C. D, E, F, G, and $H=400$ μm. Scale bar for a, b, c, d, e, f, g, and $h=100$ μm. Statistical analysis was performed with the two-way ANOVA, with a Tukey's *post hoc* test.

mice ($p<0.01$). In addition, WT+HFD+EAE and APP/PS1 + HFD+EAE mice improved their DI when comparing them with their corresponding untreated groups (WT+HFD and APP/PS1 + HFD) ($p<0.05$; $p<0.05$). Time of exploration is reported in Table 5.

Reduction in cellular glial reactivity in the brain of APP/PS1 + HFD mice treated with EAE

To evaluate the effects of EAE on the modulation of inflammatory responses, specifically, astroglia and microglial reactivity, different brain areas of WT and APP/PS1 mice fed with HFD and treated with EAE were analyzed through IHC assays. The detection for GFAP, the intermediate filament system of adult astrocytes, which is used as an astrogliosis marker, revealed a noticeable increase in the percentage of reactive tissue area in the cortex of APP/PS1 + HFD (Fig. 4 C, c) of 14.5% versus 4.5 % of WT+HFD mice ($p<0.001$, Fig. 4 in Graph I) and a reduction of astrogliosis of 14.5% in APP/PS1 + HFD (Fig. 4 C, c) versus 7.5% APP/PS1 + HFD+EAE (Fig. 4D, d, $p<0.01$, Fig. 4 in Graph I). Two-way ANOVA, genotype and treatment with EAE as factor: F(1, 12)=22,46, $p=0.0005$ for genotype; F(1, 12)=6,753, $p=0.02$ for treatment with EAE; Interaction F(1,12)=5,820, $p=0.0328$.

Meanwhile, IHC against IBA1, a protein upregulated in activated microglia, revealed an increase in APP/PS1 + HFD of 17.5% (Fig. 4 G, g) in comparison to WT+HFD with 13.6 % (Fig. 3E, e) essentially in cortical areas ($p<0.05$, Fig. 4K). In both genotypes fed with HFD (WT and APP/PS1), the treatment with EAE induced a reduction on microglial reactivity: 9.2% (WT+HFD+EAE) versus 13.3% (WT+HFD) ($p<0.05$, Fig. 4F, f versus 4E, e) and 12.4% (APP+HFD+EAE versus 17% APP+HFD+EAE) ($p<0.05$, Fig. 4 H, h versus 4 G, g). Two-way ANOVA, genotype and treatment with EAE as factor: F(1, 12)=22,46, $p=0.0005$ for genotype; F(1, 12)=6,753, $p=0.02$ for treatment with EAE; Interaction F(1,12)=5,820, $p=0.0328$.

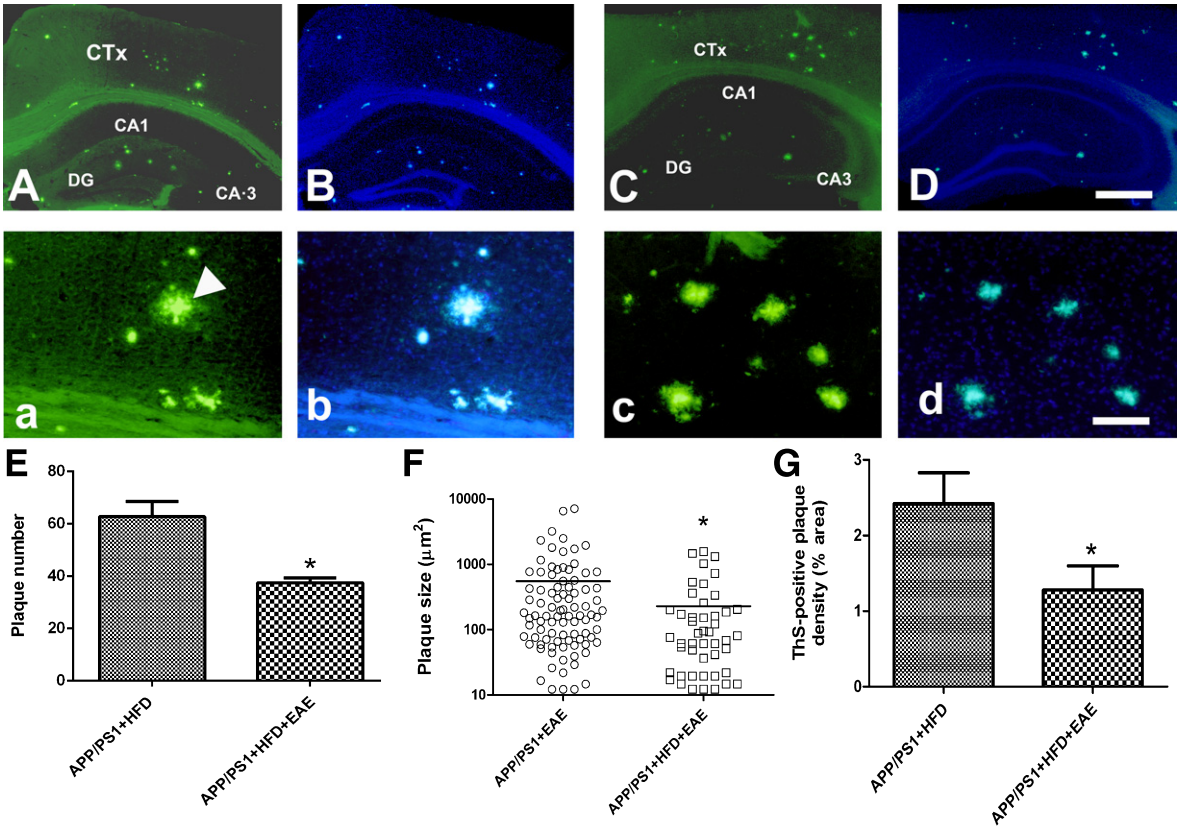

Fig. 5. Staining of Aβ plaques by ThS in the cortex and hippocampus. It was performed in APP/PS1+HFD and APP/PS1+HFD+EAE (A, B) and APP+HFD+EAE groups (B, C) and allowed the visualization of cored Aβ plaques (arrowhead; a and b). The analysis of the effect of EAE on Aβ plaques revealed that the number of the plaques were reduced in APP/PS1 + HFD treated with EAE mice as is observed in cortex (A, a versus C, c; Graph in E, $^*p < 0.05$). Also, evaluation of size plaque area (Graph in F,$^*p < 0.05$) and ThS-positive plaque density (Graph in G,$^*p < 0.05$) showed how EAE treatment reduces Aβ load. Graphs E and G represent the mean ± SEM Graph F represent mean with individual quantification values of $n = 3$/group. The statistical analysis was determined from Student *t*-test. Abbreviations: CTX, cortex; CA1, cornu ammonis 1; CA3, cornu ammonis 3; DG, Dentate gyrus. Scale bar for A, B, C and $D = 400$ μm, Scale bar a, b, c and $d = 100$ μm.

Attenuation of Aβ pathology in the APP/PS1 mouse brain treated with EAE

The ThS stain revealed Aβ deposits in cerebral cortex and hippocampus of APP/PS1 + HFD mice (Fig. 5A). The number of these deposits was reduced from an average of 67 plaques (APP+HFD) versus 37 plaques (Fig. 5E) ($p < 0.05$, Fig. 5E) and furthermore there is a reduction in the plaque size from a mean of 550 μm^2 (APP/PS1 + HFD) to 228 μm^2 (APP/PS1 + HFD+EAE) ($p < 0.05$, Fig. 5F). This effectiveness was confirmed by measuring Aβ in ThS staining and IHC against $A\beta_{1-42}$ peptide load as the percentage of the area of plaques versus total area. We observed that there was a reduction of Aβ load using ThS staining from 2.4% (APP/PS1 + HFD) to 1.27% (APP/PS1 + HFD+EAE) ($p < 0.05$, Fig. 5 G). Moreover, IHC quantification for $A\beta_{1-42}$ peptides revealed reduction of cortical Aβ load from 23% (APP/PS1 + HFD) to 18% (APP/PS1 + HFD+EAE) ($p < 0.05$, Fig. 6 C).

In addition, GFAP positive cells surrounding Aβ plaques were evaluated. A reduction of size glia surrounding Aβ plaques from 147 μm^2/cell (APP/PS1 + HFD) to 87 μm^2/cell (APP/PS1 + HFD+EAE) ($p < 0.05$, Fig. 7 G) was observed. The ratio of GFAP-area/Aβ-plaque- obtained was 3.6 APP/PS1 + HFD versus 7.0 APP/PS1 + HFD+EAE. However, statistical differences were not found ($p = 0.2380$, Fig. 7 H).

In addition, the ratio of IBA1-area/Aβ-diffuse plaque-area reflects the microglial reaction. The mean-ratio was reduced from 0.78 (APP/PS1 + HFD) to 0.29 (APP/PS1 + HFD+EAE) ($p < 0.01$, Fig. 8 G).

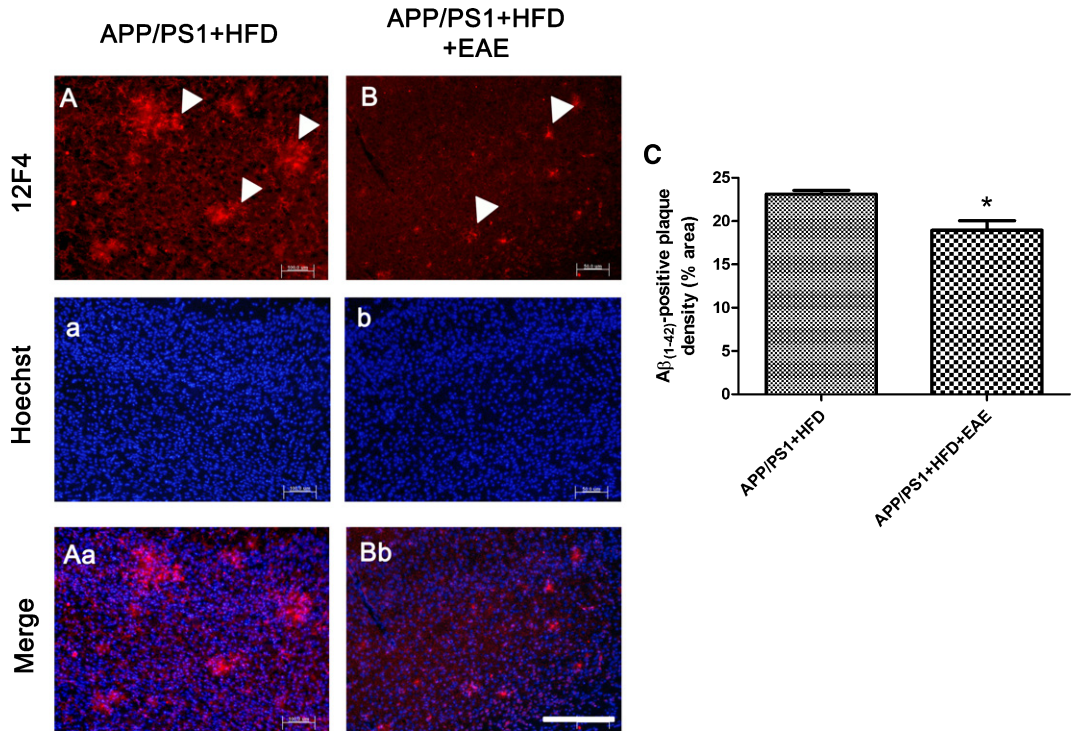

Fig. 6. Detection of $A\beta_{1-42}$ peptide in the cortex of APP/PS+HFD transgenic mice untreated and treated with EAE through fluorescent IHC assay using 12F4 antibody. Images A, a and Aa correspond to the APP/PS1 + HFD experimental group; B, b and Bb correspond to the APP/PS1 + HFD+EAE. C) $A\beta_{1-42}$ peptide depositions was evaluated as % of immunoreactive area density. EAE treatment proved effective in a decrease of % value of $A\beta_{1-42}$ ($^{*}p < 0.05$). Results were presented as mean ± SEM. Statistical analysis was performed through a Student *t*-test. Scale bar 100 μm.

DISCUSSION

EAE is composed of pentacyclic triterpenoids and different polyphenol derivatives, which have been demonstrated to have anti-inflammatory properties. The quinic acid and HHDP derivatives and similar polyphenols are a new contribution to the chemical composition of this plant [24–28].

Regarding the physiopathological conditions of AD, the polyphenols and triterpenoids found in the leaves of *U. molinae,* have indeed proved to be anti-inflammatory, anti-oxidant, and neuroprotective [38–42]. Specifically, in the present study, the beneficial effects of EAE on the amelioration of cognitive performance and improvement of some neuropathological AD biomarkers in female APP/PS1 mice fed with HFD have been demonstrated. Furthermore, previous studies reported higher abnormal Aβ production and deposition of amyloid plaques in the brain of females compared with male mice [32, 33]. Also, learning and memory loss has been described to be higher in female than males [32] and, the effects of obesogenic diet cause for an exacerbation of preclinical AD neuropathology. Thus, the positive results in the evaluation of the effects of EAE, at doses of 30 mg/kg, evidenced clearly its effectiveness as a potential new natural strategy to prevent AD [43].

The amelioration of cognitive performance and AD-related pathological features, such as neuroinflammation and Aβ deposition observed in APP/PS1 + HFD mice treated with EAE, supported that their chemical content may have therapeutic properties or preventive potential in a mixed model of preclinical T2DM and AD [44–48]. Its effects on microglial cells could explain part of the beneficial effects. Specifically, the content of EAE extracts in pentacyclic triterpenoids, such as corosolic, oleanolic/ursolic and its other triterpenoids (Table 2) which have been recognized to have anti-oxidant and anti-inflammatory properties [24–28, 39]. The identified phenolic acids, such as gallic acid, tannins, gallotannins (di-and tri-galloyl derivatives), ellagitannins (hexahydroxydiphenoyl HHDP and hexose derivatives), and for the first time identified, quinic acid

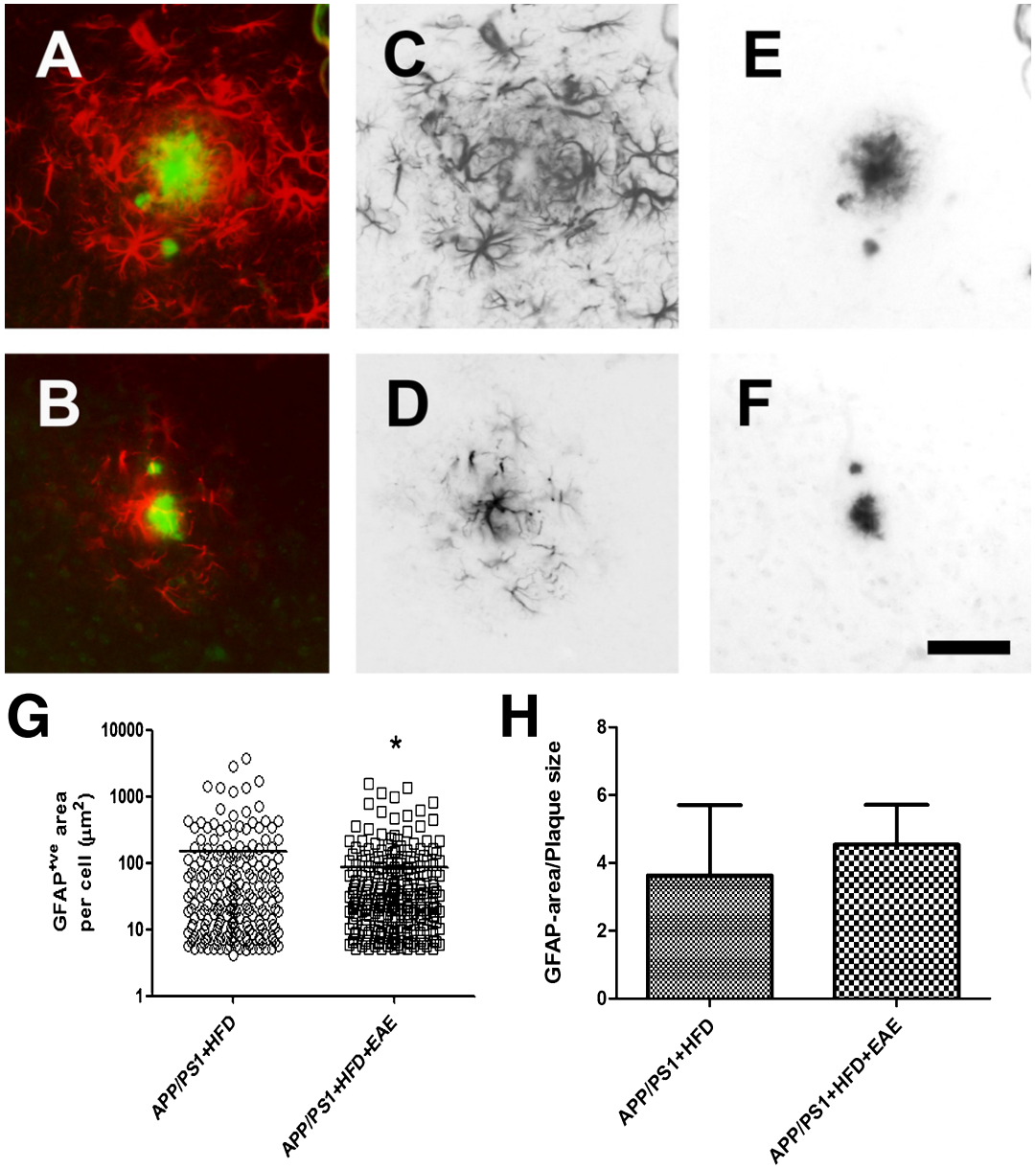

Fig. 7. Co-localization study of astrocytes surrounding Aβ depositions in the cortex of APP/PS1 + HFD (A, C, E) and APP/PS1 + HFD+EAE (B, D, F). Quantification of plaque-localized astrocyte size was performed in a 200 μm^2 field using 8-bit inverted and split channels. A and *B* = immunochemistry merged images for GFAP and ThS Staining. C and *D* = 8-bit image for GFAP and E and *G* = 8-bit image for Aβ depositions. Particle quantification was run on ImageJ software. It was observed that treatment with EAE reduces the astrocyte and plaque size ($^*p < 0.05$, H, GFAP area (μm^2)/cell), but the relationship of GFAP against of Aβ surface depositions remains unchanged (H). Results were represented as a scatter individual quantification values (Graph G) and mean ± SEM of the analysis of $n = 3$/group. Statistical analysis was performed with Student *t*-test. Scale bar = 50 μm.

derivatives (Tables 3 and 4) have also proven to be anti-inflammatory and anti-oxidant in models of neurodegenerative disease [49–51]. Although, the effect on astrocytic reaction is less patent due to the treatment does not change the area of GFAP covering a plaque and it seems that only Aβ load is decreased, our results clearly indicate that EAE has an inhibitory effect on the microglial cells reaction in the brain of APP/PS1 mice as general reactivity on the tissue as related to quantify of soluble or diffuse aggregates of $A\beta_{1-42}$ peptides. However, one of the limitations of our work has been not to evaluate the levels of

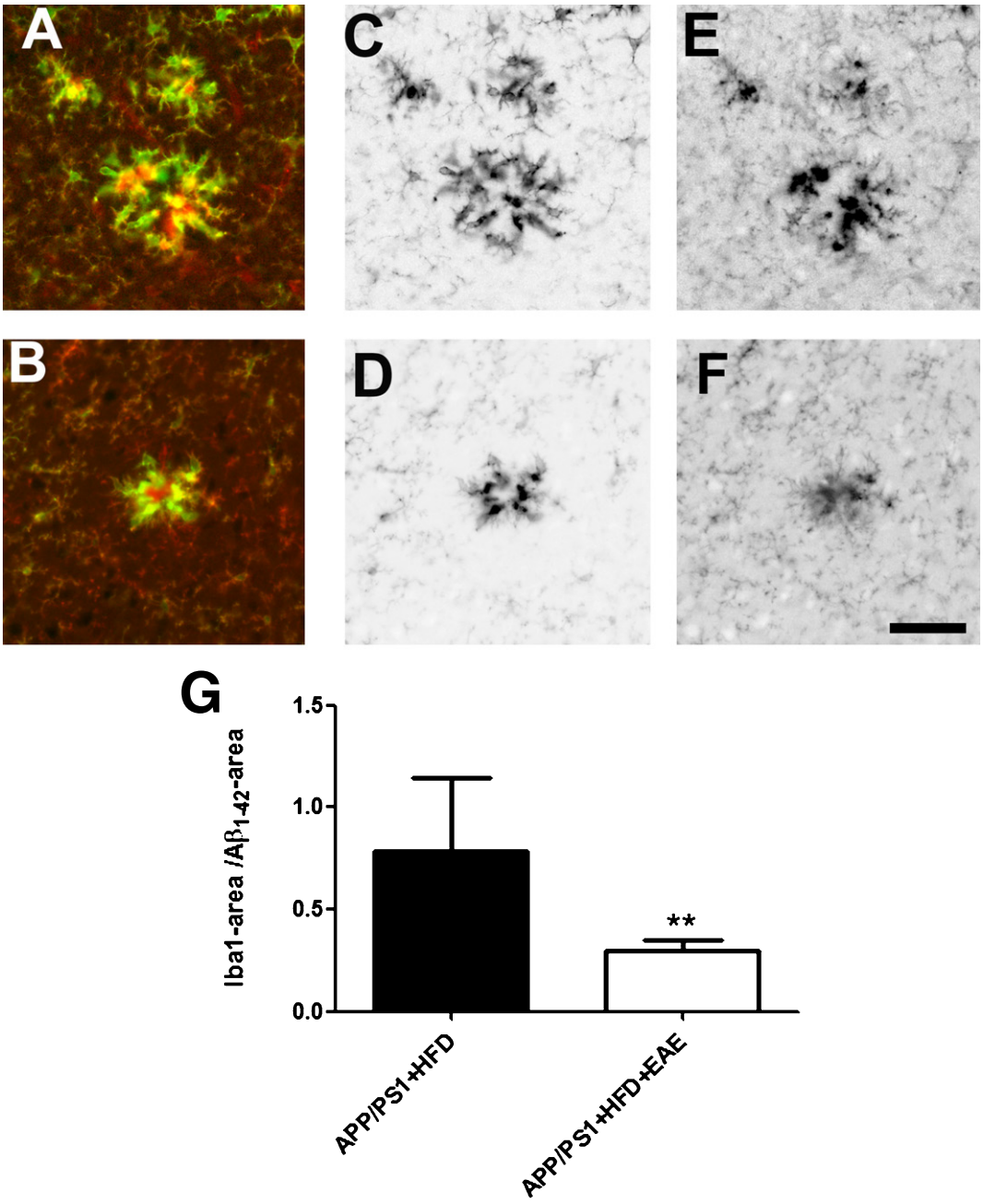

Fig. 8. Co-localization study of microglia surrounding Aβ diffuse or primitive depositions in the cortex of APP/PS1 + HFD (A, C, E) and APP/PS1 + HFD+EAE (B, D, F). The ratio of microglia reactivity (IBA1-area)/ Aβ diffuse or primitive ($A\beta_{1-42}$) was calculated. A and *B* = Immunochemistry merged images for IBA1 (green channel) and $A\beta_{1-42}$ (red channel). C and *D* = 8-bit image for IBA1 and E and *G* = 8-bit image for $A\beta_{1-42}$. It was observed that treatment with EAE reduces the ratio IB A1 β_{1-42} ($^{**}p < 0.01$, G). Results were represented mean ± SEM. Statistical analysis was performed with Student *t*-test. Scale bar = 50 μm.

proinflammatory cytokines or enzymes involved in the inflammatory process such as cyclooxygenase-2 activity.

Moreover, the action of polyphenols has been associated with the prevention and treatment of dementia; supporting the results obtained in our study with the NORT that demonstrated the improvement in cognitive capabilities in WT+HFD and APP/PS1 + HFD mice treated with EAE. Other compounds present in EAE are flavonoids, such as quercetin, myricetin,

kaempferol, epicatechin/catechin (Tables 3 and 4) which showed beneficial effects against Aβ neurotoxicity [43]. The resulting data is in accordance with previous reported research that linked chronic treatment with anti-inflammatory drugs and improvement of AD models [52–55].

Nowadays, the exact etiology of AD is not fully clear, however, the amyloid hypothesis states that overproduction of soluble Aβ and aggregations of this peptide in the brain are primary responsible causes for the progression of the disease [10–14]. Thus, targeting Aβ reduction mechanisms and its aggregation is believed to be a possibly suitable strategy to improve the pathology [52–57]. It has been reported that the main component of diffuse plaques or pre-plaques are $A\beta_{42}$ peptides probably the most pathologic in AD [10–14, 56–68]. In this way, EAE compounds have shown to modulate Aβ aggregation [56, 63–68]. Specifically, several phenols as digalloyl hexose, gallic acid, epicatechin/catechin, quercetin pentoside and ellagic acid, have been shown to both modulate amyloid oligomers aggregation and to protect from the neurotoxic consequences of their release [64–79]. The reduction of Aβ deposits with EAE administration supported this hypothesis [64]. On this point, reduction of microglia reactivity by EAE could be the result of a decrease in Aβ plaques.

In conclusion, the findings of this study demonstrate that the chemical composition of EAE has neuroprotective effects, observed in a mixed model of preclinical T2DM and AD (APP/PS1 + HFD) model. Obtained data suggested that improvement in cognitive functions is due to a microglial and astrocytic reactivity reduction, together with a decrease in Aβ plaque formation. Also, note that EAE improved peripheral parameters related to the process of obesity. Considering the reported relationship between obesity and cognitive loss, the effect of EAE on metabolism could also contribute to the beneficial effect of the extract in this preclinical model of AD. Posterior studies must be conducted to establish the mechanisms of how the compounds found in the EAE from *U. molinae* leaves are able to recover cognition and pathological parameters of AD, since it would be a novel potential therapeutic agent to prevent this neurodegenerative disease.

ACKNOWLEDGMENTS

This work was supported by the Spanish Ministry of Science and Innovation SAF2017-84283-R, PI2016/01, CB06/05/0024 (CIBERNED) and the European Regional Development Founds. Research team from UB and URV belongs to 2014SGR-525 from Generalitat de Catalunya. Thesis Support Grant CONICYT-CHILE-21130380 (Daniela Jara-Moreno). FONDECYT-CHILE- 1130155 FONDAP 15130011. Postdoctoral Fellowship to Rubén D. Castro-Torres (No. 298337, CONACYT-MEXICO) in cooperation for consolidating research groups (Doctoral Program in Sciences in Molecular Biology in Medicine, LGAC Molecular Bases of Chronic-Degenerative Diseases and its Applications 000091, PNPC, CONACYT-MEXICO).

Authors' disclosures available online (https://www.j-alz.com/manuscript-disclosures/18-0174r2).

REFERENCES

[1] Alzheimer's Association (2016) 2016 Alzheimer's disease facts and figures. *Alzheimers Dement* **12**, 459-509.

[2] Masters CL, Bateman R, Blennow K, Rowe CC, Spearling RA, Cummings JL (2015) Alzheimer's disease. *Nat Rev Dis Primers* **1**, 15056.

[3] Livingston G, Sommerlad A, Orgeta V, Costafreda SG, Huntley J, Ames D, Mukadam N (2017) Dementia prevention, intervention, and care. *Lancet* **140**, 31363-3136.

[4] Jahn H (2013) Memory loss in Alzheimer's disease. *Dialogues Clin Neurosci* **15**, 445-454.

[5] Querfurth HW, LaFerla FM (2010) Alzheimer's disease. *N Engl J Med* **362**, 329-344.

[6] Yiannopoulou KG, Papageorgiou SG (2013) Current and future treatments for Alzheimer's disease. *Ther Adv Neurol Disord* **6**, 19-33.

[7] Chneider LS, Mangialasche F, Andreasen N, Feldman H, Giacobini E, Jones R, Mantua V, Mecocci P, Pani L, Winblad B, Kivipelto M (2014) Clinical trials and late-stage drug development for Alzheimer's disease: An appraisal from 1984 to 2014. *J Intern Med* **275**, 251-283.

[8] Cummings J, Lee G, Mortsdorf T, Ritter A, Zhong K (2017) Alzheimer's disease drug development pipeline: 2017. *Alzheimers Dement (N Y)* **3**, 367-384.

[9] Soejitno A, Tjan A, Purwata TE (2015) Alzheimer's disease: Lessons learned from amyloidocentric clinical trials. *CNS Drugs* **29**, 487-502.

[10] Hardy JA, Higgins GA (1992) Alzheimer's disease: The amyloid cascade hypothesis. *Science* **256**, 184-185.

[11] Hardy JA, Selkoe DJ (2002) The amyloid hypothesis of Alzheimer's disease: Progress and problems on the road to therapeutics. *Science* **297**, 353-356.

[12] Walsh DM, Selkoe DJ (2007) Abeta oligomers—a decade of discovery. *J Neurochem* **101**, 1172-1184.

[13] Selkoe DJ, Hardy J (2016) The amyloid hypothesis of Alzheimer's disease at 25 years. *EMBO Mol Med* **8**, 595-608.

[14] Viola KL, Klein WL (2015) Amyloid β oligomers in Alzheimer's disease pathogenesis, treatment, and diagnosis. *Acta Neuropathol* **129**, 183-206.

[15] Heneka MT, Carson MJ, El Khoury J, Landreth GE, Brosseron F, Feinstein DL, Jacobs AH, Wyss-Coray T, Vitorica J, Ransohoff RM, Herrup K, Frautschy SA, Finsen

B, Brown GC, Verkhratsky A, Yamanaka K, Koistinaho J, Latz E, Halle A, Petzold GC, Town T, Morgan D, Shinohara ML, Perry VH, Holmes C, Bazan NG, Brooks DJ, Hunot S, Joseph B, Deigendesch N, Garaschuk O, Boddeke E, Dinarello CA, Breitner JC, Cole GM, Golenbock DT, Kummer MP (2015) Neuroinflammation in Alzheimer's disease. *Lancet Neurol* **14**, 388-405.

[16] Wyss-Coray T, Rogers J (2012) Inflammation in Alzheimer disease-a brief review of the basic science and clinical literature. *Cold Spring Harb Perspect Med* **2**, a006346.

[17] Ardura-Fabregat A, Boddeke EWGM, Boza-Serrano A, Brioschi S, Castro-Gomez S, Ceyzériat K, Dansokho C, Dierkes T, Gelders G, Heneka MT, Hoeijmakers L, Hoffmann A, Iaccarino L, Jahnert S, Kuhbandner K, Landreth G, Lonnemann N, Löschmann PA, McManus RM, Paulus A, Reemst K, Sanchez-Caro JM, Tiberi A, Van der Perren A, Vautheny A, Venegas C, Webers A, Weydt P, Wijasa TS, Xiang X, Yang Y (2017) Targeting neuroinflammation to treat Alzheimer's disease. *CNS Drugs* **31**, 1057-1082.

[18] Zhu S, Wang J, Zhang Y, He J, Kong J, Wang JF, Li XM (2017) The role of neuroinflammation and amyloid in cognitive impairment in an APP/PS1 transgenic mouse model of Alzheimer's disease. *CNS Neurosci Ther* **23**, 310-320.

[19] Cifuentes D, Poittevin M, Dere E, Broquères-You D, Bonnin P, Benessiano J, Pocard M, Mariani J, Kubis N, Merkulova-Rainon T, Lévy BI (2015) Hypertension accelerates the progression of Alzheimer-like pathology in a mouse model of the disease. *Hypertension* **65**, 218-224.

[20] Kalaria RN, Maestre GE, Arizaga R, Friedland RP, Galasko D, Hall K, Luchsinger JA, Ogunniyi A, Perry EK, Potocnik F, Prince M, Stewart R, Wimo A, Zhang ZX, Antuono P, World Federation of Neurology Dementia Research Group (2008) Alzheimer's disease and vascular dementia in developing countries: Prevalence, management, and risk factors. *Lancet Neurol* **7**, 812-826.

[21] Janson J, Laedtke T, Parisi JE, O'Brien P, Petersen RC, Butler PC (2004) Increased risk of type 2 diabetes in Alzheimer disease. *Diabetes*, **53**, 474-481.

[22] Reitz C (2013) Dyslipidemia and the risk of Alzheimer's Disease. *Curr Atheroscler Rep* **15**, 1-14.

[23] Vanhanen, M., Koivisto, K, Moilanen L, Helkala EL, Hänninen T, Soininen H, Kervinen K, Kesäniemi YA, Laakso M, Kuusisto J (2006) Association of metabolic syndrome with Alzheimer disease: A population-based study. *Neurology* **67**, 843-847.

[24] Aguirre MC, Delporte C, Backhouse N, Erazo S, Letelier ME, Cassels BK, Silva X, Alegría S, Negrete R (2006) Topical anti-inflammatory activity of 2 alpha-hydroxy pentacyclic triterpene acids from the leaves of Ugni molinae. *Bioorg Med Chem* **14**, 5673-5677.

[25] Peña-Cerda M, Arancibia-Radich J, Valenzuela-Bustamante P, Pérez-Arancibia R, Barriga A, Seguel I, García L, Delporte C (2017) Phenolic composition and antioxidant capacity of Ugni molinae Turcz. leaves of different genotypes. *Food Chem* **215**, 219-227.

[26] Delporte C, Backhouse N, Inostroza V, Aguirre MC, Peredo N, Silva X, Negrete R, Miranda HF (2007) Analgesic activity of Ugni molinae (murtilla) in mice models of acute pain. *J Ethnopharmacol* **112**, 162-165.

[27] Rubilar M, Pinelo M, Ihl, M, Scheuermann E, Sineiro J, Nunez MJ (2006) Murta leaves (Ugni molinae Turcz) as a source of antioxidant polyphenols. *J Agr Food Chem* **54**, 59-64.

[28] Goity L, Queupil MJ, Jara D, Alegria MSP, Barriga A, Aguirre MC, Delporte C (2013) An HPLC-UV and HPLC-ESI_MS based method for identification of anti-inflammatory triterpenoids from the extracts of Ugni molinae. *Bol Latinoam Caribe Plantas Med Aromát* **12**, 108-116.

[29] Zhang S, Chai R, Yang YY, Guo SQ, Wang S, Guo T, Xu SF, Zhang YH, Wang ZY, Guo C (2017) Chronic diabetic states worsen Alzheimer neuropathology and cognitive deficits accompanying disruption of calcium signaling in leptin-deficient APP/PS1 mice. *Oncotarget* **8**, 43617-43634.

[30] Ruiz HH, Chi T, Shin AC, Lindtner C, Hsieh W, Ehrlich M, Gandy S, Buettner C (2016) Increased susceptibility to metabolic dysregulation in a mouse model of Alzheimer's disease is associated with impaired hypothalamic insulin signaling and elevated BCAA levels. *Alzheimers Dement* **12**, 851-861.

[31] Ramos-Rodriguez JJ, Spires-Jones T, Pooler AM, Lechuga-Sancho AM, Bacskai BJ, Garcia-Alloza M (2017) Progressive neuronal pathology and synaptic loss induced by prediabetes and type 2 diabetes in a mouse model of Alzheimer's disease. *Mol Neurobiol* **54**, 3428-3438.

[32] Jiao SS, Bu XL, Liu YH, Zhu C, Wang QH, Shen LL, Liu CH, Wang YR, Yao XQ, Wang YJ (2016) Sex dimorphism profile of Alzheimer's disease-type pathologies in an APP/PS1 mouse model. *Neurotox Res* **29**, 256-266.

[33] Li X, Feng Y, Wu W, Zhao J, Fu C, Li Y, Ding Y, Wu B, Gong Y, Yang G, Zhou X (2016) Sex differences between APPswePS1dE9 mice in A-beta accumulation and pancreatic islet function during the development of Alzheimer's disease. *Lab Anim* **50**, 275-285.

[34] Ennaceur A, Neave N, Aggleton JP (1997) Spontaneous object recognition and object location memory in rats: The effects of lesions in the cingulate cortices, the medial prefrontal cortex, the cingulum bundle and the fornix. *Exp Brain Res* **113**, 509-519.

[35] Michodjehoun-Mestres L1, Amraoui W, Brillouet JM (2009) Isolation, characterization, and determination of 1-O-trans-cinnamoyl-beta-D-glucopyranose in the epidermis and flesh of developing cashew apple (Anacardium occidentale L.) and four of its genotypes. *J Agric Food Chem* **57**, 1377-1382.

[36] Paxinos G, Watson C (1986) *The Rat Brain in Stereotaxic Coordinates*, Academic Press, Sydney.

[37] De Lemos L, Junyent F, Camins A, Castro-Torres RD, Folch J, Olloquequi J, Beas-Zarate C, Verdaguer E, Auladell C (2018) Neuroprotective effects of the absence of JNK1 or JNK3 isoforms on kainic acid-induced temporal lobe epilepsy-like symptoms. *Mol Neurobiol* **55**, 4437-4452.

[38] Stohs SJ, Miller H, Kaats GR (2012) A review of the efficacy and safety of banaba (Lagerstroemia speciosa L.) and corosolic acid. *Phyt Res* **26**, 317-324.

[39] Molino S, Dossena M, Buonocore D, Ferrari F, Venturini L, Ricevuti G, Verri M (2016) Polyphenols in dementia: From molecular basis to clinical trials. *Life Sci* **161**, 69-77.

[40] Kajdzanoska M, Petreska J, Stefova M (2011) Comparison of different extraction solvent mixtures for characterization of phenolic compounds in strawberries. *J Agr Food Chem* **59**, 5272-5278.

[41] Bhullar KS, Rupasinghe HP (2013) Polyphenols: Multipotent therapeutic agents in neurodegenerative diseases. *Oxid Med Cell Longev* **2013**, 891748.

[42] Vauzour D (2012) Dietary polyphenols as modulators of brain functions: Biological actions and molecular mechanisms underpinning their beneficial effects. *Oxid Med Cell Longev* **2012**, 914273.

[43] McDade E, Bateman RJ (2017) Stop Alzheimer's before it starts. *Nature* **547**, 153-155.

[44] Eng LF, Ghirnikar RS, Lee YL (2000) Glial fibrillary acidic protein: GFAP-thirty-one years (1969-2000). *Neurochem Res* **25**, 1439-1451.

[45] Pekny M, Wilhelmsson U, Pekna M (2014) The dual role of astrocyte activation and reactive gliosis. *Neurosci Lett* **565**, 30-38.

[46] Mosher KI, Wyss-Coray T (2014) Microglial dysfunction in brain aging and Alzheimer's disease. *Biochem Pharmacol* **88**, 594-604.

[47] Ettcheto M, Petrov D, Pedrós I, Alva N, Carbonell T, Beas-Zarate C, Pallas M, Auladell C, Folch J, Camins A (2016) Evaluation of neuropathological effects of a high-fat diet in a presymptomatic Alzheimer's disease stage in APP/PS1 mice. *J Alzheimers Dis* **54**, 233-251.

[48] Petrov D, Pedrós I, Artiach G, Sureda FX, Barroso E, Pallás M, Auladell C, Folch J, Camins A (2015) High-fat diet-induced deregulation of hippocampal insulin signaling and mitochondrial homeostasis deficiencies contribute to Alzheimer disease pathology in rodents. *Biochem Biophys Acta* **1852**, 1687-1699.

[49] Fragoulis A, Siegl S, Fendt M, Jansen S, Soppa U, Brandenburg LO, Wruck CJ (2017) Oral administration of methysticin improves cognitive deficits in a mouse model of Alzheimer's disease. *Redox Biol* **12**, 843-853.

[50] Mani V, Jaafar S M, Azahan NSM, Ramasamy K, Lim SM, Ming L C, Majeed ABA (2017) Ciproxifan improves cholinergic transmission, attenuates neuroinflammation and oxidative stress but does not reduce amyloid level in transgenic mice. *Life Sci* **180**, 23-35.

[51] Mori T, Koyama N, Tan J, Segawa T, Maeda M, Town T (2017) Combination therapy with octyl gallate and ferulic acid improves cognition and neurodegeneration in a transgenic mouse model of Alzheimer disease. *J Biol Chem* **292**, 11310-11325.

[52] McGeer PL, Guo JP, Lee M, Kennedy K, McGeer EG (2018) Alzheimer's disease can be spared by nonsteroidal anti-inflammatory drugs. *J Alzheimers Dis* **62**, 1219-1222.

[53] Morrison JH, Baxter MG (2012) The ageing cortical synapse: Hallmarks and implications for cognitive decline. *Nat Rev Neurosci* **13**, 240-250.

[54] Krause DL, Müller N (2010) Neuroinflammation, microglia and implications for anti-inflammatory treatment in Alzheimer's disease. *Int J Alzheimers Dis* **2010**, 73280.

[55] Becher A, Drenckhahn A, Pahner I, Margittai M, Jahn R, Ahnert-Hilger G (1999) The synaptophysin-synaptobrevin complex: A hallmark of synaptic vesicle maturation. *J Neurosci* **19**, 1922-1931.

[56] Zhang W, Hao J, Liu R, Zhang Z, Lei G, Su C, Miao J, Li Z (2011) Soluble Aβ levels correlate with cognitive deficits in the 12-month-old APPswe/PS1dE9 mouse model of Alzheimer's disease. *Behav Brain Res* **222**, 342-350.

[57] Jankowsky JL, Zheng H (2017) Practical considerations for choosing a mouse model of Alzheimer's disease. *Mol Neurodegener* **12**, 89.

[58] Ban JY, Nguyen HTT, Lee HJ, Cho SO, Ju HS, Kim JY, Seong YH (2008) Neuroprotective properties of gallic acid from Sanguisorbae radix on amyloid beta protein (25-35)-induced toxicity in cultured rat cortical neurons. *Biol Pharmaceut Bull* **31**, 149-153.

[59] Choi Y, Kim TD, Paik SR, Jeong K, Jung S (2008) Molecular simulations for anti-amyloidogenic effect of flavonoid myricetin exerted against Alzheimer's β-amyloid fibrils formation. *Bull Korean Chem Soc* **29**, 1505-1509.

[60] Cuevas E, Limón D, Pérez-Severiano F, Díaz A, Ortega L, Zenteno E, Guevara J (2009) Antioxidant effects of epicatechin on the hippocampal toxicity caused by amyloid-beta 25-35 in rats. *Eur J Pharmacol* **616**, 122-127.

[61] Murphy MP, LeVine H (2010) Alzheimer's disease and the amyloid-β peptide. *J Alzheimers Dis* **19**, 311-323.

[62] Re F, Airoldi C, Zona C, Masserini M, Ferla B L, Quattrocchi N, Nicotra F (2010) Beta amyloid aggregation inhibitors: Small molecules as candidate drugs for therapy of Alzheimer's disease. *Curr Med Chem* **17**, 2990-3006.

[63] Roher A, Wolfe D, Palutke M, KuKuruga D (1986) Purification, ultrastructure, and chemical analysis of Alzheimer disease amyloid plaque core protein. *Proc Nat Acad Sci U S A* **83**, 2662-2666.

[64] Torok B, Bag S, Sarkar M, Dasgupta S, Torok M (2013) Structural features of small molecule amyloid-beta self-assembly inhibitors. *Curr Bioact Com* **9**, 37-63.

[65] Zhao J, O'Connor T, Vassar R (2011) The contribution of activated astrocytes to Aβ production: Implications for Alzheimer's disease pathogenesis. *J Neuroinflammation* **8**, 150.

[66] Fiori J, Naldi M, Bartolini M, Andrisano V (2012) Disclosure of a fundamental clue for the elucidation of the myricetin mechanism of action as amyloid aggregation inhibitor by mass spectrometry. *Electrophoresis* **33,** 3380-3386.

[67] Ono K, Yoshiike Y, Takashima A, Hasegawa K, Naiki H, Yamada M (2003) Potent anti – amyloidogenic and fibril – destabilizing effects of polyphenols *in vitro*: Implications for the prevention and therapeutics of Alzheimer's disease. *J Neurochem* **87**, 172-181.

[68] Jiménez-Aliaga K, Bermejo-Bescós P, Benedí J, Martín-Aragón S (2011) Quercetin and rutin exhibit antiamyloidogenic and fibril-disaggregating effects *in vitro* and potent antioxidant activity in APPswe cells. *Life Sci* **89**, 939-945.

[69] Planchard MS, Samel MA, Kumar A, Rangachari V (2012) The natural product betulinic acid rapidly promotes amyloid-β fibril formation at the expense of soluble oligomers. *ACS Chem Neurosci* **3**, 900-908.

[70] Porat Y, Abramowitz A, Gazit E (2006) Inhibition of amyloid fibril formation by polyphenols: Structural similarity and aromatic interactions as a common inhibition mechanism. *Chem Biol Drug Des* **67**, 27-37.

[71] Sylla T, Pouységu L, Da Costa G, Deffieux D, Monti JP, Quideau S (2015) Gallotannins and tannic acid: First chemical syntheses and *in vitro* inhibitory activity on Alzheimer's amyloid β-peptide aggregation. *Angew Chem* **127**, 8335-8339.

[72] Hong SY, Jeong WS, Jun M (2012) Protective effects of the key compounds isolated from Corni fructus against β-amyloid-induced neurotoxicity in PC12 cells. *Molecules* **17**, 10831-10845.

[73] Kim H, Park BS, Lee KG, Choi CY, Jang SS, Kim YH, Lee SE (2005) Effects of naturally occurring compounds on fibril formation and oxidative stress of β-amyloid. *J Agr Food Chem* **53,** 8537-8541.

[74] Oliveira MR (2016) The effects of ellagic acid upon brain cells: A mechanistic view and future directions. *Neurochem Res* **41**, 1219-1228.

[75] Guimaraes CC, Oliveira DD, Valdevite M, Saltoratto AL, Pereira, SLV, de Castro França S, Pereira PS (2015) The glycosylated flavonoids vitexin, isovitexin, and quercetrin isolated from Serjania erecta Radlk (Sapindaceae) leaves

protect PC12 cells against amyloid-β 25-35 peptide-induced toxicity. *Food Chem Toxicol* **86**, 88-bor94.

[76] Heo HJ, Lee CY (2005) Epicatechin and catechin in cocoa inhibit amyloid β protein induced apoptosis. *J Agr Food Chem* **53**, 1445-1448.

[77] Kim MJ, Seong AR, Yoo JY, Jin CH, Lee YH, Kim YJ, Yoon HG (2011) Gallic acid, a histone acetyltransferase inhibitor, suppresses β-amyloid neurotoxicity by inhibiting microglial-mediated neuroinflammation. *Mol Nutr Food Res* **55**, 1798-1808.

[78] Latruffe N (2017) Resveratrol and grape extract-loaded solid lipid nanoparticles for the treatment of Alzheimer's disease. *Molecules* **22**, E277.

[79] Michodjehoun-Mestres L, Souquet JM, Fulcrand H, Bouchut C, Reynes M, Brillouet JM (2009) Monomeric phenols of cashew apple (Anacardium occidentale L.). *Food Chem* **112**, 851-857.